Dalton Transactions

Accepted Manuscript

ROYAL SOCIETY OF CHEMISTRY

www.rsc.org/dalton

Cite this: DOI: 10.1039/c0xx00000x

www.rsc.org/xxxxxx

ARTICLE TYPE

Employment of triketone to construct dysprosium(III) single-molecule magnet

Chao Wang,[a] Shuang-Yan Lin,[a] Jianfeng Wu,[a,b] Sen-Wen Yuan[a] and Jinkui Tang*[a]

Received (in XXX, XXX) Xth XXXXXXXXX 20XX, Accepted Xth XXXXXXXXX 20XX

DOI: 10.1039/b000000x

The initial employment of triketone ligand in 4f coordination chemistry afforded a series of dinuclear complexes. The magnetic studies revealed that antiferromagnetic interaction exists in digadolinium(III) compound, while the dysprosium(III) constructed complex exhibits single-molecule magnet (SMM) behaviour at low temperature with energy barrier of 86.8 K.

Introduction

The design of new single-molecule magnets (SMMs) has long been of great interest in the race for high energy barrier (ΔE_a) and blocking temperature (T_B) SMMs.[1] In recent years, a growing amount of literatures have been demonstrated that the key factors of SMMs lie in paramagnetic sources and suitable crystal fields of central ions.[2] To date, the best candidate of the former factor is Dy(III) ion, which exhibits a Karmers ground state of $^6H_{15/2}$, and has been employed to construct various kind of SMMs.[3] While, the crystal fields mostly depend on local symmetry of coordination spheres. More recently, a special class of β-diketonate lanthanide complexes that possess SMMs behavior with large energy barriers were presented based on Dy ions with the composition of Dy(β-diketonate)$_3$[cap/$(H_2O)_2$], where cap stands for capping ligands.[4] It was structurally confirmed that the β-diketonates in these compounds act as both chelating ligands *via* two oxygen atoms and matched anions, and the central Dy ions were situated in an approximate D_{4d} local symmetry, enabling the compounds functioning as SMM.

This kind of single-ion magnets (SIMs) containing Dy ions usually exhibit large energy barriers and high blocking temperature, both of which are crucial for the advancement of single-molecule data storage and processing technologies.[1c,1d] Given the remarkable progress of β-diketonate-Dy strategies, we wonder whether the ΔE_a or T_B can be significantly enhanced *via* the combination of two β-diketonate-Dy moieties, which possess excellent SIM properties.[4] In this regard, to extend SMMs from mononuclear to dinuclear while maintaining the local symmetry as much as possible seems to be an appealing task to us. The simplest, as well as the most efficient approach is the addition of carbonyl group to β-diketonate ligand. With this in mind, in this paper, we selected 1,1,1,7,7,7-hexafluoroheptane-2,4,6-trione (H_2hfht) as primary ligand and 1,10-phenanthrene (phen) as capping ligand to construct new SMMs.

Experimental Section

General. All starting materials were commercial available and at least A.R. Grade. All solvents were purified using standard methods and redistilled before use. 1,1,1,7,7,7-hexafluoroheptane-2,4,6-trione (H_2hfht) was synthesized according to the literature reported and after slightly modification.[5] Fourier transform IR (FTIR) spectra were recorded with a Thermo Scientific Nicolet 6700 spectrophotometer with ATR module using the reflectance technique (4000-600 cm^{-1}). The purities of polycrystalline samples adopted in magnetic measuring were confirmed by IR spectra and elemental analysis. All magnetization data were recorded on a Quantum Design MPMS-XL SQUID magnetometer equipped with a 7 T magnet. The variable-temperature magnetization was measured with an external magnetic field of 1000 Oe in the temperature range of 2-300 K and frequency dependent *ac* susceptibility was measured with an oscillating field of 3.0 Oe The experimental magnetic susceptibility data are corrected for the diamagnetism estimated from Pascal's constants. Powder X-ray diffraction measurements of complexes **3**-**9** were recorded on Bruker D8 advance X-Ray diffractometer using CuKα radiation.

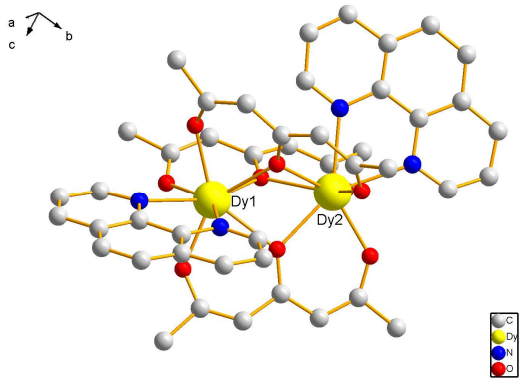

Fig. 1 Molecular structure of $Dy_2(hfht)_3(phen)_2$ (**1**), disordered fluorine atoms and hydrogen atoms are omitted for clarity.

Synthesis of complex $Dy_2(hfht)_3(phen)_2$ (1): 75 mg H_2hfht (0.3 mmol) was added to a 25 mL methanol solution containing 91.2 mg (0.2 mmol) $Dy(NO_3)_3·5H_2O$ with continuous stirring. After

that, 0.6 mL triethylamine in methanol (1.0 mol·L^{-1}) was added to this mixture, and followed by 39.0 mg (0.2 mmol) phen monohydrate. The resulting solution was stirring for one hour and filtered, the filtrate was allowed to stand at room temperature for one week. Block-shaped crystals suitable for single crystal analysis were formed by slow evaporation of solvent and collected by careful filtration. Yield: 104.6 mg (73.2%). IR spectra (cm^{-1}): 1615(s), 1551(s), 1536(w), 1495(s), 1424(m), 1389(w), 1347(w), 1269(vs), 1184(vs), 1114(vs), 1037(vw), 985(s), 886(s), 864(w), 844(m), 819(s), 778(w), 755(w), 722(s). Elemental analysis found (calc)% for complex **1**: C: 37.45 (37.81) H: 1.57 (1.55) N: 3.86 (3.92).

Synthesis of complexes 2-10 ($Ln_2(hfht)_3(phen)_2$ Ln = Nd(**2**), Sm(**3**), Eu(**4**), Gd(**5**), Tb(**6**), Ho(**7**), Er(**8**), Tm(**9**), Yb(**10**))**:** Complexes **2-10** were synthesized according to a similar process of complex **1**, using corresponding lanthanide nitrate hydrate as starting materials instead of $Dy(NO_3)_3·5H_2O$. IR spectra and elemental analysis data of these nine complexes are provided in Supporting Information.

Table 1 Crystallographic parameters of complexes **1**, **2** and **10.**

Compound name	**1**	**2**	**10**
Chemical formula	$C_{45}H_{22}Dy_2F_{18}N_4O_9$	$C_{45}H_{22}F_{18}N_4Nd_2O_9$	$C_{45}H_{22}F_{18}N_4O_9Yb_2$
Formula Mass	1429.66	1393.14	1450.74
a/Å	12.076(3)	11.241(2)	12.0714(6)
b/Å	29.138(6)	11.485(2)	29.1600(14)
c/Å	13.369(3)	21.149(4)	13.3336(7)
α/°	90	75.515(3)	90
β/°	92.286(4)	74.784(4)	92.2480(10)
γ/°	90	67.553(3)	90
Unit cell volume/Å^3	4700.4(18)	2400.6(8)	4689.8(4)
Temperature/K	296(2)	296(2)	296(2)
Space group	*P*21/n	*PT*	*P*21/n
No. of formula units per unit cell, *Z*	4	2	4
Absorption coefficient, *μ*/mm^{-1}	3.287	2.269	4.096
No. of reflections measured	26591	15156	29005
No. of independent reflections	8418	9487	9214
R_{int}	0.1408	0.0229	0.0375
Final R_1 values ($I > 2\sigma(I)$)	0.0859	0.0332	0.0294
Final $wR(F^2)$ values ($I > 2\sigma(I)$)	0.2112	0.0688	0.0597
Final R_1 values (all data)	0.1537	0.0506	0.0426
Final $wR(F^2)$ values (all data)	0.2688	0.0787	0.0649
Goodness of fit on F^2	0.984	1.015	1.024

Table 2 The range of bond lengths in complexes **1**, **2** and **10.**

	(Ln-N) /Å	(Ln-O) /Å
Complex **2** (Nd)	2.586-2.642	2.294-2.560
Complex **1** (Dy)	2.501-2.562	2.229-2.452
Complex **10** (Yb)	2.474-2.528	2.199-2.423

X-ray Crystallography: Single-crystal X-ray diffraction measurements of the title complexes were carried out on a Bruker Apex II CCD diffractometer with graphite monochromated MoKα radiation (λ = 0.71073Å) at 293 K. The structures were solved by direct methods and refined on F^2 with full-matrix least-squares techniques using SHELXL-2013 programs. The locations of lanthanide atoms were easily determined, oxygen, nitrogen, and carbon atoms were subsequently determined from the difference Fourier maps. Anisotropic thermal parameters were assigned to all non-hydrogen atoms. Severely disordered fluorine atoms in trifluoromethyl groups were divided into two parts, some restrains (ISOR, DFIX, SIMU) were used in refinement to bring these molecules into reasonable models. The hydrogen atoms were introduced in calculated positions and refined with a fixed geometry with respect to their carrier atoms. Crystallographic data and refinement details are given in Table 1. CCDC 1000270 (**2**), 1000271 (**1**) and 1000272 (**10**) contain the supplementary crystallographic data for this paper. These data can be obtained free of charge from the Cambridge Crystallographic Data Centre via www.ccdc.cam.ac.uk/data_request/cif.

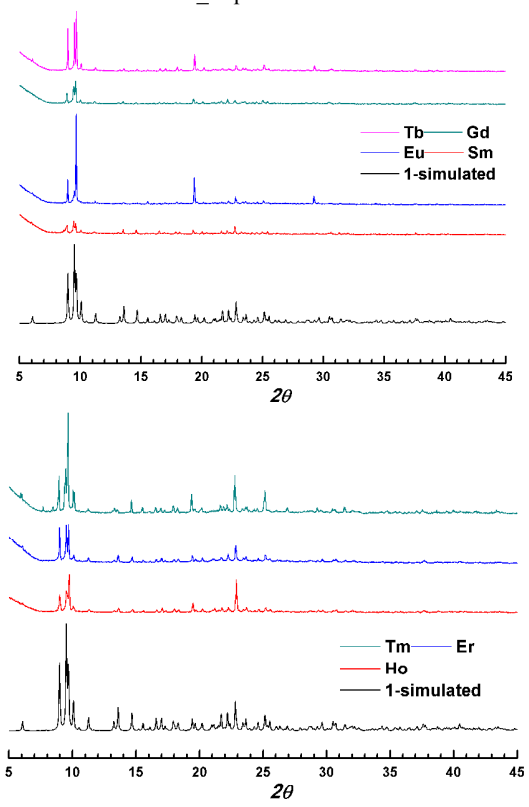

Fig. 2 Powder XRD analysis of complexes **3-6** (top) and **7-9** (bottom). The black line is simulated data from single crystal data of **1**.

Results and Discussion

Crystal Structure. According to single-crystal X-Ray diffraction analysis, complex **1** crystallizes in monoclinic space group *P*21/n, possessing a dinuclear unit. As shown in Fig. 1, one molecule of complex **1** consists of two central Dy ions, three hfht dianion moieties and two chelating phen ligands. The hfht dianion act as a doubled bidentate ligand, linking two Dy ions together. Each Dy ion is eight-coordinated by six oxygen atoms from hfht moieties with Dy-O bonds lengths in the range of 2.229-2.452 Å, and two nitrogen atoms from one capping phen ligand with Dy-N bond lengths from 2.501 to 2.562 Å, which is comparable to previously reported complexes.[4a,4c] The coordination sphere of Dy1 ion can

be described as square antiprism, while Dy2 ion is situated in distorted dodecahedron with triangular faces.[6] Within this molecule, two Dy ions are connected by three μ_2-O atoms coming from three hfht dianions with the Dy···Dy intramolecular length of 3.650 Å, while the shortest Dy···Dy intermolecular distance is 8.800 Å (Fig. S1). In addition, this dinuclear unit is surrounded by the severely disordered fluorine atoms of the trifluoromethyl groups, and consequently each dinuclear unit is well isolated. The atoms in hfht moieties, except fluorine atoms, are nearly coplanar, indicating a strong conjugated nature of the hfht dianions.

For complex **2**, the replacement of Nd ion made the space group changed from *P*21/n to *P*-1. However, the unsymmetric unit remains similar to Dy_2 aggregate of complex **1**, except for some tiny changes in bond lengths and angles owing to the radius' difference of lanthanide ions. As listed in Table 2, the bond lengths of both Ln-O and Ln-N decrease with the sequence of Nd, Dy and Yb, which can be attributed to the lanthanide contraction.[3j] As shown in Fig. 2 and S2-S8, the structures of complexes **3**-**9** are identified well by powder X-ray diffraction, the coincidences between the experimental peak positions and simulated patterns of complex **1** strongly suggest that these seven complexes are isomorphic to complexes **1** and **10**.

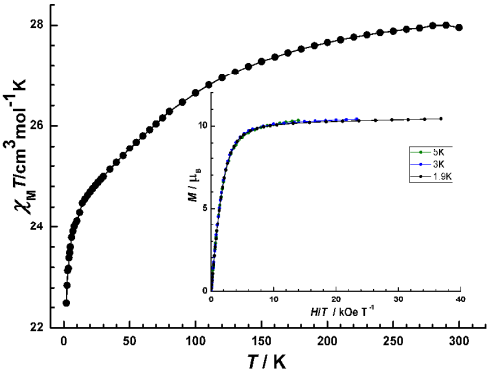

Fig. 3 The $\chi_M T$ versus T curve for complex **1**, the inset is magnetization curves for complex **1** at the temperature of 1.9, 3.0 and 5.0 K, respectively.

Static magnetic properties of 1. The temperature dependence of the magnetic susceptibilities in the form of $\chi_M T$ versus T plots for complex **1** in the temperature range of 300-2.0 K are shown in Figure **3**. At room-temperature, the observed $\chi_M T$ value is 27.95 cm^3 K mol^{-1}, which shows agreement with two uncoupled Dy ions in $^6H_{15/2}$ ground state with g = 4/3 (28.35 cm^3 K mol^{-1}).[7] On cooling, the $\chi_M T$ value decreases smoothly, which could ascribe to the depopulation of Stark sub-levels and/or antiferromagnetic interactions between two Dy ions.[3b,8] Below 50 K, it begins to decrease sharply and reaches a minimum of 22.48 cm^3 K mol^{-1} at 2.0 K.

The magnetization curves of complex **1** in the field range of 0-70 kOe at different temperatures are shown in inset of Fig. 3. The maximum value at 1.9 K reaches 10.43 μ_B, which is far from the saturation value (20 μ_B) and possible due to the crystal-field effects and the low-lying excited states.[3a] Furthermore, M versus H/T curves at different temperature do not show coincidence at high field range, indicating the presence of magnetic anisotropy in Dy ion.[9]

Static magnetic properties of 5. In order to study the magnetic coupling between the two metal ions in this unit, Gd ions with the absence of orbital angular momentum are introduced to replace the anisotropic Dy ions. Isostructural complex $Gd_2(hfht)_3(phen)_2$ (**5**), identified by powder XRD analysis, was obtained and its temperature dependence of the magnetic susceptibilities were also measured under 1000 *dc* field in the temperature range of 300-2.0 K. As shown in Fig. 4, at room temperature, the observed $\chi_M T$ value is 15.92 cm^3 K mol^{-1}, which is slightly higher than two uncoupled Gd(III) ions (f^7 electron configuration, g = 2.00, $\chi_M T$ = 7.88 cm^3 K mol^{-1}). With the decreasing temperature, the $\chi_M T$ value essentially keeps as a constant above 20 K, and begins to sharply decrease and reaches a minimum of 9.83 cm^3 K mol^{-1} at 2.0 K. Magnetization curve for complex **5** at 1.9 K is also shown in inset of Figure **4**, possessing a saturated value of 14.05 μ_B, which coincides well with the theoretical value 14.00 μ_B (g = 2.00).

The *dc* magnetic behavior of complex **5** was quantitatively analyzed by adopting the spin Hamiltonian $\hat{\boldsymbol{H}} = -2J\hat{\boldsymbol{S}}_{Gd1}\hat{\boldsymbol{S}}_{Gd2} + g\beta H(\hat{\boldsymbol{S}}_{Gd1} + \hat{\boldsymbol{S}}_{Gd2})$. Best fit to this experimental data provided us with the parameters of g = 2.02 and J = -0.058 cm^{-1} (R^2 = 0.9982). The negative J value indicates weak antiferromagnetic coupling between two Gd(III) ions.

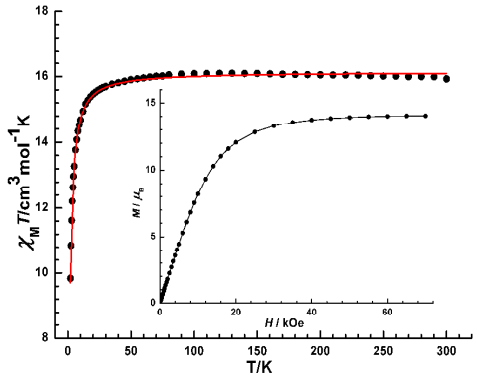

Fig. 4 The $\chi_M T$ versus T curve for complex **5**, the red line is the best simulation with the parameter of g = 2.02, J = - 0.058cm^{-1}, the inset is magnetization curve for complex **5** at 1.9 K, showing saturation value of approximate 14.0 μ_B.

Static magnetic properties of other complexes. Fig. 5 presents the $\chi_M T$ versus T curves of the rest complexes. As listed in Table 3, the $\chi_M T$ values at room temperature agree well with their corresponding theoretical ones. Like the magnetic properties of complex **1**, the $\chi_M T$ values of all complexes descend more or less with the decreasing of temperature, which also ascribe to the depopulation of lanthanide's Stark sub-levels.

For complex **3**, in which the Sm ion's first or even higher excited state $^6H_{7/2}$, $^6H_{9/2}$, ···, $^6H_{15/2}$ can be obviously populated at room temperature,[10] the $\chi_M T$ value observed at room temperature is significant larger than the theoretical one. On cooling, $\chi_M T$ value decreases continuously to a minimum of 0.062 cm^3 K mol^{-1} at 2.0 K. Assuming that the effect of crystal fields are negligible, the magnetic susceptibilities can be treated as a function with the spin-orbit coupling parameter λ and molecular field parameter zj', which roughly stand for the magnetic exchange of two Sm ions within one molecule. The best simulation (Fig. S9) in the temperature range of 50-300 K provided us with the parameters of λ = 224.3 cm^{-1}, g = 0.33, zj' = -2.68 cm^{-1}, the negative zj' value

indicates antiferromagnetic coupling between two Sm ions.

Similar to complex **3**, complex **4**, which should be diamagnetic according to the ground state $^7F_0$ (J = 0) of Eu ions, exhibits a nonzero $\chi_M T$ value of 2.935 cm^3 K mol^{-1} at room temperature, indicating a thermal population on the exited state of $^7F_1$, $^7F_2$, ⋯, $^7F_6$. While the gradual decline of the $\chi_M T$ value on cooling ascribes to the thermal depopulation of the excited states. The best simulation in the whole temperature range gives us the parameters of λ = 346.9 cm^{-1}, g = 0.79, zj' = 1.38 cm^{-1} (Fig. S10). This positive zj' value suggests that ferromagnetic interaction between two Eu ions may exist in this compound.

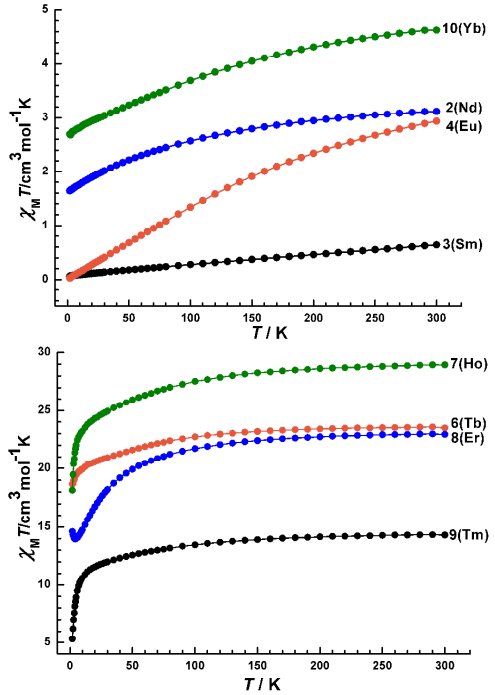

Fig. 5 Temperature dependence of $\chi_M T$ versus T plots at 1000 Oe for **2**-**4**, **10** (top) and **6**-**9** (bottom).

Table 3. Experimental value of $\chi_M T$ at 300 K for complexes **2**-**4**, and **6**-**10**

Complex	Complex **2**	Complex **3**
Theoretical value (cm^{3}Kmol^{-1})	3.28	0.188
Experimental (cm^{3}Kmol^{-1})	3.12	0.639
Complex	Complex **4**	Complex **6**
Theoretical value (cm^{3}Kmol^{-1})	~3.1	23.62
Experimental (cm^{3}Kmol^{-1})	2.935	23.49
Complex	Complex **7**	Complex **8**
Theoretical value (cm^{3}Kmol^{-1})	28.12	22.95
Experimental (cm^{3}Kmol^{-1})	28.94	22.90
Complex	Complex **9**	Complex **10**
Theoretical value (cm^{3}Kmol^{-1})	14.30	5.14
Experimental (cm^{3}Kmol^{-1})	14.31	4.63

In these anisotropic dinuclear compounds, three factors may influence the thermal evolution of $\chi_M T$ values: Firstly, the depopulation of m_j levels on lowering the temperature should be the primary contributor to the decline of the $\chi_M T$ value at high temperature range. Secondly, the intramolecular magnetic coupling between the two lanthanide ions *via* three μ_2-O atoms affect the $\chi_M T$ value significantly at low temperature. Thirdly, through the space, there may also exist intermolecular interactions, but should be rather weak and negligible because the dinuclear aggregates are well isolated. As shown in Fig. 5, below 5 K, the $\chi_M T$ value of complex **8** increases with the decreasing temperature at low temperature, which is possibly due to the presence of ferromagnetic interaction between two Er ions.

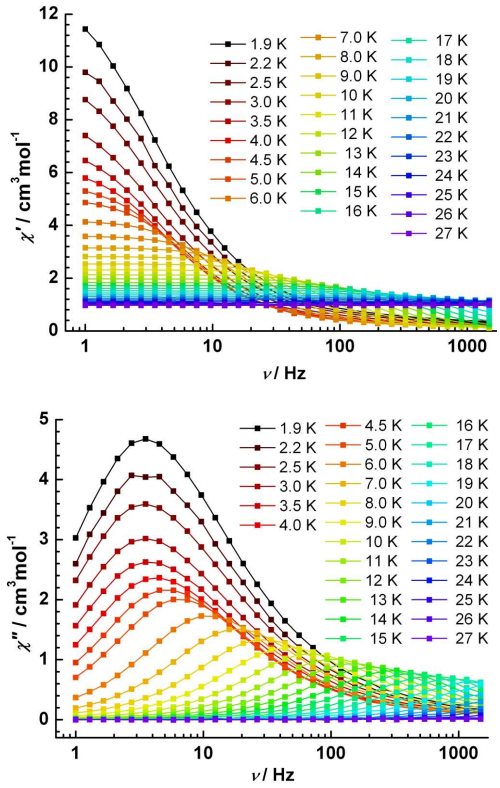

Fig. 6 Frequency dependence of the real (top) and imaginary (bottom) components of the ac magnetic susceptibilities for **1** under zero dc field in the temperature range of 1.9-27 K. The lines are guides for the eyes.

Dynamic magnetic properties of 1. The frequency dependence of *ac* susceptibility for complex **1** was carried out at the temperature range of 1.9-27 K under zero *dc* field. As shown in Fig. 6, below 17 K, the imaginary components exhibit obvious peak values that vary with frequency and these peaks move gradually to high frequency as the temperature increases.

The magnetization relaxation times in the form of lnτ, derived from ac measurements, versus T^{-1} are listed in Fi. 7. Fitting these data on high temperature range using Arrhenius law provided us the energy barrier of 86.8 K and the pre-exponential factor τ_0 = 1.17×10^{-7} s, that is comparable to mononuclear complexes based on Dy ion and various kinds β-diketonates. Below 3.0 K, the relaxation times keep as a constant around 4.5×10^{-2} s, which indicates a pure quantum regime in low temperature range and also explains why obvious hysteresis loop could not be observed with the sweeping rate of a traditional magnetometer.[4b,4c]

The *ac* data in the form of Cole-Cole plots of complex **1** are shown in Figure **8**, where each curve shows almost semi-circular shape. Generalized Debye model are employed to fit these data and the obtained α values drop in the range of 0.04-0.25, which strongly suggests SMM behavior.[11] Furthermore, as temperature increases from 3.0 to 13 K, the fitted α value are also decreased gradually from 0.167 to 0.025.

The dynamic magnetic properties of other anisotropic

dinuclear complexes were also measured under zero dc field at the frequency of 1000 Hz (Fig. S11-S18). However, on obvious out-of-phase *ac* signals were observed for these complexes.

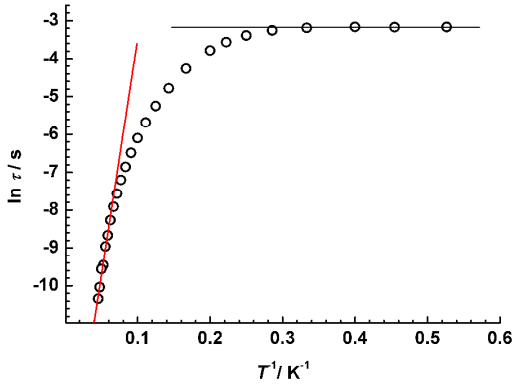

Fig. 7 lnτ vs. T^{-1} plot for **1** under zero dc field. The red line is fitted with the Arrhenius law.

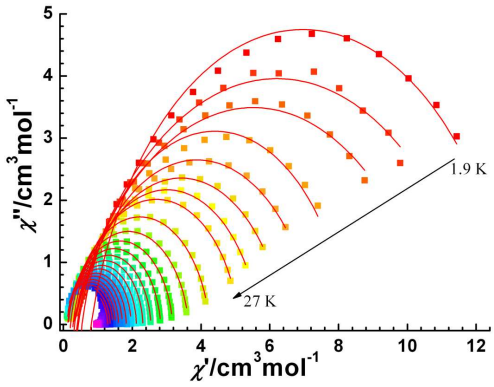

Fig. 8 Cole–Cole plots of **1** under zero dc field in the temperature range of 1.9-27 K. The red lines are the best fits with an extended Debye model.

Conclusions

In summary, in our efforts to rationally design SMMs, the initial employment of fluorine substituted triketone in 4f coordination chemistry has yielded a new family of dinuclear complexes. To our best knowledge, these are the first series of lanthanide complexes based on triketone ligand. Complex **1** exhibits SMMs behavior with energy barrier of 86.8 K. The present study demonstrates the potential of the completely unexplored triketone ligand in the design of 4f SMMs. The use of triketone has been indicated as a promising strategy thanks to its excellent chelating and bridging abilities and will definitely initiate further studies towards the rational design of SMMs using polyketones and their derivatives.

Acknowledgment

We thank the National Natural Science Foundation of China (Grants 21371166, 21331003 and 21221061) for financial support.

Notes and references

[a] *State Key Laboratory of Rare Earth Resource Utilization, Changchun Institute of Applied Chemistry, Chinese Academy of Sciences, Changchun 130022, P. R. China, E-mail: tang@ciac.ac.cn*

[b] *University of Chinese Academy of Sciences, Beijing, 100049, P. R. China*

† Electronic Supplementary Information (ESI) available: Selected bond lengths and angles of complexes **1**, **2** and **10** are listed in **Tables S1-S3**. The packing arrengment of complex **1** is listed in Fig. S1. IR spectra and elemental analysis data of complexes **2-10** are also listed in Supporting Information. The powder XRD patterns for **3-9** are presented in Fig. S2-S8. The simulations of complexes **3** and **4** are presented in Fig. S9 and S10, respectively. The dynamic magnetic properties of complex **3-10** are presented in Fig. S11-S18. See DOI: 10.1039/b000000x/

1 (a) R. Sessoli, D. Gatteschi, A. Caneschi and M. A. Novak, *Nature* 1993, **365**, 141; (b) M. Murrie, *Chem. Soc. Rev.* 2010, **39**, 1986; (c) D. N. Woodruff, R. E. P. Winpenny and R. A. Layfield, *Chem. Rev.* 2013, **113**, 5110; (d) P. Zhang, Y.-N. Guo and J. Tang, *Coord. Chem. Rev.* 2013, **257**, 1728; (e) N. Ishkawa, M. Sugita, T. Ishikawa, S. Koshihara and Y, Kaizu, *J. Am. Chem. Soc.* 2003, **125**, 8694; (f) F. Branzoli, P. Carretta, M. Filibian, G. Zoppellaro, M. J. Graf, J. R. Galan-Mascaros, O. Fuhr, S. Brink and M. Ruben, *J. Am. Chem. Soc.* 2009, **131**, 4387; (g) M. Gonidec, D. Amabilino and J. Veciana, *Dalton Trans.* 2012, **41**, 13632; (h) N. Ishikawa, M. Sugita, N. Tanaka, T. Ishikawa, S. Koshihara and Y. Kaizu, *Inorg. Chem.* 2004, **43**, 5498.

2 (a) R. Sessoli and A. K. Powell, *Coord. Chem. Rev.* 2009, **253**, 2328; (b) L. Sorace, C. Benelli and D. Gatteschi, *Chem. Soc. Rev.* 2011, **40**, 3092; (c) X. H. Yi, K. Bernot, F. Pointillart, G. Poneti, G. Calvez, C. Daiguebonne, O. Guillou and R. Sessoli, *Chem. Eur. J.* 2012, **18**, 11379; (d) K. C. Mondal, A. Sundt, Y. H. Lan, G. E. Kostakis, O. Waldmann, L. Ungur, L. F. Chibotaru, C. E. Anson and A. K. Powell, *Angew. Chem.-Int. Ed.* 2012, **51**, 7550; (e) S. Cardona-Serra, J. M. Clemente-Juan, E. Coronado, A. Gaita-Arino, A. Camon, M. Evangelisti, F. Luis, M. J. Martinez-Perez and J. Sese, *J. Am. Chem. Soc.* 2012, **134**, 14982; (f) M. A. AlDamen, J. M. Clemente-Juan, E. Coronado, C. Marti-Gastaldo and A. Gaita-Arino, *J. Am. Chem. Soc.* 2008, **130**, 8874; (g) M. A. AlDamen, S. Cardona-Serra, J. M. Clemente-Juan, E. Coronado, A. Gaita-Arino, C. Marti-Gastaldo, F. Luis and O. Montero, *Inorg. Chem.* 2009, **48**, 3467.

3 (a) J. Tang, I. Hewitt, N. T. Madhu, G. Chastanet, W. Wernsdorfer, C. E. Anson, C. Benelli, R. Sessoli and A. K. Powell, *Angew. Chem.-Int. Ed.* 2006, **45**, 1729; (b) Y.-N. Guo, G.-F. Xu, P. Gamez, L. Zhao, S.-Y. Lin, R. Deng, J. Tang and H.-J. Zhang, *J. Am. Chem. Soc.* 2010, **132**, 8538; (c) I. J. Hewitt, J. Tang, N. T. Madhu, C. E. Anson, Y. Lan, J. Luzon, M. Etienne, R. Sessoli and A. K. Powell, *Angew. Chem.-Int. Ed.* 2010, **49**, 6352; (d) R. J. Blagg, C. A. Muryn, E. J. L. McInnes, F. Tuna, and R. E. P. Winpenny, *Angew. Chem.-Int. Ed.* 2011, **50**, 6530; (e) Y.-N. Guo, G.-F. Xu, W. Wernsdorfer, L. Ungur, Y. Guo, J. Tang, H.-J. Zhang, L. F. Chibotaru and A. K. Powell, *J. Am. Chem. Soc.* 2011, **133**, 11948; (f) J. Long, F. Habib, P. H. Lin, I. Korobkov, G. Enright, L. Ungur, W. Wernsdorfer, L. F. Chibotaru and M. Murugesu, *J. Am. Chem. Soc.* 2011, **133**, 5319; (g) D. P. Mills, F. Moro, J. McMaster, J. van Slageren, W. Lewis, A. J. Blake and S. T. Liddle, *Nat Chem* 2011, **3**, 454; (h) S.-Y. Lin, W. Wernsdorfer, L. Ungur, A. K. Powell, Y.-N. Guo, J. Tang, L. Zhao, L. F. Chibotaru and H.-J. Zhang, *Angew. Chem.-Int. Ed.* 2012, **51**, 12767; (i) L. Ungur, S. K. Langley, T. N. Hooper, B. Moubaraki, E. K. Brechin, K. S. Murray and L. F. Chibotaru, *J. Am. Chem. Soc.* 2012, **134**, 18554; (j) D. Aguilà, L. A. Barrios, V. Velasco, L. Arnedo, N. Aliaga-Alcalde, M. Menelaou, S. J. Teat, O. Roubeau, F. Luis and G. Aromí, *Chem. -Eur. J.* 2013, **19**, 5881.

4 (a) G.-J. Chen, C.-Y. Gao, J.-L. Tian, J. Tang, W. Gu, X. Liu, S.-P. Yan, D.-Z. Liao and P. Cheng, *Dalton Trans.* 2011, **40**, 5579; (b) G. J. Chen, Y. N. Guo, J. L. Tian, J. K. Tang, W. Gu, X. Liu, S. P. Yan, P. Cheng and D. Z. Liao, *Chem. Eur. J.* 2012, **18**, 2484; (c) Y. Bi, Y. N. Guo, L. Zhao, Y. Guo, S. Y. Lin, S. D. Jiang, J. K. Tang, B. W. Wang and S. Gao, *Chem. Eur. J.* 2011, **17**, 12476; (d) S. D. Jiang, B. W. Wang, G. Su, Z. M. Wang and S. Gao, *Angew. Chem.-Int. Ed.* 2010, **49**, 7448; (e) X.-L. Wang, L.-C. Li and D.-Z. Liao, Inorg. Chem. 2010, **49**, 4735; (f) X.-L. Mei, Y. Ma, L.-C. Li and D.-Z. Liao, *Dalton Trans.* 2012, **41**, 505; (g) X.-L. Li, C.-L. Chen, Y.-L. Gao, C.-M. Liu, X.-L. Feng, Y.-H. Gui and S.-M. Fang, *Chem.–Eur. J.* 2012, **18**, 14632; (h) D.-P. Li, X.-P. Zhang, T.-W. Wang, B.-B. Ma, C.-H. Li, Y.-Z. Li and X.-Z. You, *Chem. Commun.* 2011, **47**, 6867; (i) D.-

P. Li, T.-W. Wang, C.-H. Li, D.-S. Liu, Y.-Z. Lin and X.-Z. You, *Chem. Commun*. 2010, **46**, 2929; (j) P. Hu, X.-F. Wang, Y. Ma, Q.-L. Wang, L.-C. Li and D.-Z. Liao, *Dalton Trans.* 2014, **43**, 2234.

5 D. V. Sevenard, O. Kazakova, D. L. Chizhov and G.-V. Röschenthaler, *J. Fluorine Chem*. 2006, **127**, 983.

6 (a) D. Casanova, M. Llunell, P. Alemany and S. Alvarez, *Chem. Eur. J.* 2005, **11**, 1479; (b) S. Alvarez, P. Alemany, D. Casanova, J. Cirera, M. Llunell and D. Avnir, *Coord. Chem. Rev.* 2005, **249**, 1693; (c) D. Casanova, J. Cirera, M. Llunell, P. Alemany, D. Avnir and S. Alvarez, *J. Am. Chem. Soc.* 2004, **126**, 1755; (d) M. Pinsky and D. Avnir, *Inorg. Chem.* 1998, **37**, 5575.

7 (a) C. Benelli and D. Gatteschi. *Chem. Rev.* 2002, **102**, 2369; (b) R. L. Carlin. *Magnetochemisty* Springer Berlin 1986.

8 B. Hussain, D. Savard, T. J. Burchell, W. Wernsdorfer and M. Murugesu, *Chem. Commun*. 2009, 1100.

9 (a) S. Kanegawa, S. Karasawa, M. Maeyama, M. Nakano and N. Koga, *J. Am. Chem. Soc.* 2008, **130**, 3079; (b) P.-H. Lin, T. J. Burchell, R. Clérac and M. Murugesu, *Angew. Chem. Int. Ed.* 2008, **47**, 8848; (c) A. Okazawa, Y. Nagaichi, T. Nogami and T. Ishida, *Inorg. Chem.* 2008, **47**, 8859.

10 (a) Y. Hinatsu and Y. Doi, *Bull. Chem. Soc. Jpn*. 2003, **76**, 1093; (b) J.-X. Xu, Y. Ma, D.-Z. Liao, G.-F. Xu, J. Tang, C. Wang, N. Zhou, S.-P. Yan, P. Cheng and L.-C. Li, *Inorg. Chem.* 2009, **48**, 8890.

11 (a) S. M. J. Aubin, Z. M. Sun, L. Pardi, J. Krzystek, K. Folting, L. C. Brunel, A. L. Rheingold, G. Christou and D. N. Hendrickson, *Inorg. Chem.* 1999, **38**, 5329; (b) K. S. Cole and R. H. Cole, *J. Chem. Phys.* 1941, **9**, 341.

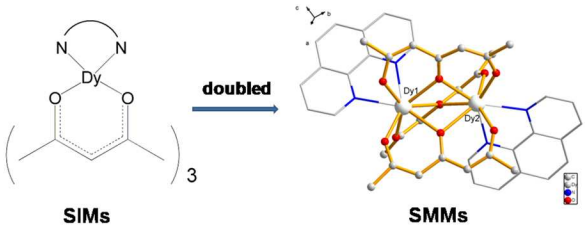

The use of completely unexplored triketone ligand in 4f coordination chemistry has afforded a new dinuclear dysprosium(III) SMM.